JNCS
Journal of Nepal Chemical Society July 2024, Vol. 44, No. 2, 43-51
ISSN: 2091-0304 (print)
DOI: https://doi.org/10.3126/jncs.v44i2.68302
RESEARCH ARTICLE

Mechanical and Structural Characterization of Resole Resin Composites Reinforced with *Sabai* Grass-Derived Cellulose Fibers

Aabha Puri[1], Rameshwar Adhikari[2], Rajesh Pandit[1]*

[1]*Department of Chemistry, Tri-Chandra Multiple Campus, Ghantaghar, Kathmandu, Nepal*

[2]*Research Centre for Applied Science and Technology (RECAST), Tribhuvan University, Kirtipur 44618, Kathmandu, Nepal*

*Corresponding E-mail: *rajesh.pandit@trc.tu.edu.np*

(Received: May 9, 2024; revised: July 7, 2024; accepted: July 15, 2024)

Abstract

Cellulose fibers were extracted from *Sabai* grass (*Eulaliopsis binata*) using mechanical and chemical treatments. The grass was ground to ~250 μm powder and bleached with hydrogen peroxide and acetic acid. The bleached fibers were treated with 6% sodium hydroxide solution and incorporated into resole resin at various weight percentages to prepare the composites. The prepared samples were characterized by X-ray Diffraction (XRD), Fourier Transform Infra-Red (FTIR) spectroscopy, Scanning Electron Microscopy (SEM), and compressive strength tests. The XRD and FTIR showed a nanometric crystallite size of 3.84 nm and effective removal of non-cellulosic compounds, respectively, leading to a compressive strength increase from 15.60 MPa to 25.26 MPa at 3 wt.-% cellulose fiber. The compressive strength improved up to 3 wt.-% cellulose fiber, which however declined upon adding more filler. SEM revealed modified surface morphology in the composites with cellulose fibers.

Keywords: *Sabai* grass; Cellulose fibers; Resole composites; Compressive strength;

Introduction

Cellulose, discovered and isolated over 150 years ago by Anselme Payen, is the most abundant renewable, high molecular weight linear polysaccharide composed of β-1-4 glucopyranose units [1, 2]. It is found in the cell walls of plants, bacteria, fungi, algae, and tunicates, known for its excellent mechanical properties, high absorbance, and insulating properties [3]. Various plants, including bamboo, wheat straw, maize stalk, and sisal fiber, are sources of cellulose. Sabai grass (*Eulaliopsis binata*), a perennial plant grown mainly in China, and some South Asian and Asia-Pacific countries, is a notable cellulose source [4]. This grass is valued for its high fiber quality and production, easy plantation, good perennial growth, wide adaptability, stress resistance, well-developed root system, and dense populating propensity. Its excellent flexibility and strength, high leaf fiber content (>55%), low lignin content (<14%), and average fiber length (~20mm) make it ideal for paper production, rayon, woven materials, and filler materials in plastics and mud matrix [5].

Resole resins are condensation polymers obtained by condensing phenol with formaldehyde in the presence of an alkaline catalyst while novolac resins are synthesized in an acidic catalyst. These resins are solid, insoluble, rigid materials after curing, exhibiting high thermal and mechanical stability, high strength, fire resistance, low toxicity, and excellent insulating properties. Phenolic resoles

thus useful thermosetting materials for manufacturing composite panels based on wood, like plywood [5]. Cellulose fibers with superior mechanical properties can be added to polymers like phenol-formaldehyde resins in varying proportions to create a novel eco-friendly composite material with improved mechanical strength [6, 7].

A composite is a multiphase solid material where a filler is incorporated into the polymer matrix to enhance structural and functional performance [8]. The cellulose fiber-enhanced phenol-formaldehyde resin can produce a superior and eco-friendly bio composite with excellent mechanical properties. [9, 10]. These composites can be synthesized through methods like intercalation of polymer or pre-polymer from solution, *in-situ* intercalative polymerization, melt intercalation, direct mixing of polymer and particulates, *in-situ* polymerization, and sol-gel process. The production can be optimized regarding temperature, pressure, and molding time [11]. Further work on different formaldehyde-to-phenol ratios and cellulose weight percentages was noted, where the resole synthesis involves a molar excess of formaldehyde ($1<f/p<3$) [12]. Their study considered three reaction sequences for composite synthesis: the addition of formaldehyde and cellulose to phenol, chain growth or pre-polymer formation, and crosslinking or curing reaction [12]. The main reason for utilizing cellulose in composites is to exploit its high strength and Young's modulus, originating from the crystalline nature of cellulose molecules due to hydrogen bonds along the molecular chains. The main challenge in preparing cellulose nanocomposites is their poor dispersion in the polymer matrix due to fibril agglomeration from hydrogen bonding within the cellulose fibrils [12].

To improve interfacial bonding, various surface treatments like alkali treatment [13], silane treatment [14], acetylation [15], and different coupling agents [16] have been attempted, with alkali treatment being the most effective. This treatment increases hydrophobicity, and surface roughness, and reduces water uptake [13-16]. The traces of degraded lignin and hemicellulose in chemically treated cellulose fiber enhance the matrix-fiber interface and increase the effective surface area available for resin wetting due to the separation of fibers [17]. This paper explores the use of extracted cellulose fiber for preparing resole resin/cellulose fiber composites in different wt.-% and investigates their mechanical properties, such as compressive strength, for mechanical use. Therefore, this study aims to isolate cellulose fibers from *Sabai* grass and incorporate them into resole resin to prepare and characterize eco-friendly composites with enhanced mechanical properties

Materials and Methods

Materials

The *Sabai* grass sample was collected from Pyuthan district. The chemical reagents (Phenol: 98%, molecular weight of 94.11 g/mol, formaldehyde: 99%, molecular weight of 30.03 g/mol, and sodium hydroxide: 98%, molecular weight of 40.00 g/mol), manufactured by LOBA Chemie Pvt. Ltd., Mumbai, India, were purchased from local suppliers in Kathmandu. All the chemicals (AR grade) were used without further purification.

Collection and Preparation of *Sabai* Grass

The collected *Sabai* grass sample was sun-dried for 3-4 days to transition its green color to greenish yellow. The sample was then thoroughly washed with water to remove impurities and dried to eliminate moisture. Long

fibers of the *Sabai* grass were chopped into small pieces and ground into a powder with a particle size of less than 250 µm. This powder was then sieved using a sieve with mesh size a 250 µm pore diameter.

Isolation of Cellulose from *Sabai* Grass Powder

The cellulose isolation process involved bleaching and alkaline treatment. The bleaching solution was prepared by mixing hydrogen peroxide and 99.8 wt.-% glacial acetic acid. The required amount of *Sabai* grass fiber powder was weighed, immersed in the bleaching solution in a round-bottom flask, and heated to 130 °C for 3 hr. After cooling, the bleached product was filtered using suction filtration, rinsed with deionized water until a pH of 7 was achieved, and dried at 70 °C for 24 hr. The bleached *Sabai* grass fiber was then immersed in an alkaline solution to remove pectin and hemicelluloses, using a 6 wt.-% sodium hydroxide solution at room temperature. This mixture was heated to 80 °C for 2 hr. with simultaneous stirring at 150 rpm using a magnetic stirrer for 8 hr. The mixture was washed with deionized water until a pH of 7 was achieved, then dried at room temperature for 48 hours, followed by oven drying at 60 °C for 18 hr. Finally, the white cellulose fiber powder was collected in a beaker.

Preparation of Resole/Cellulose Composites

For pure resole, a phenol-formaldehyde mixture (1:3) was combined with sodium hydroxide, used as a catalyst, and heated with stirring on a hot plate at 90 °C. Once the mixture became viscous and turned pinkish brown, it was carefully transferred into a grease-coated cubic mold. For the preparation of composites, cellulose was added to the viscous resole. Different amounts of cellulose fibers (1 %, 2 %, 3 %, 5 %, and 10 % by weight of resole resin) were used. The prepared samples were pre-cured at 60 °C for 24 hr. and post-cured at 100 °C for 12 hr. in an oven, resulting in a hard, infusible, and clear pinkish-brown solidified resole resin and composite product.

Characterization and Testing

The isolated cellulose fiber from *Sabai* grass and the resole/cellulose composites were characterized using XRD (Bruker D2 Phaser diffractometer, USA) with a monochromatic CuKα radiation source (λ = 0.15418 nm) at angle 2θ ranging from 10° - 80°. FTIR (IR Affinity-2500, Shimadzu, Japan) with a wavenumber range of 4000-500 cm^{-1}, and SEM (JEOL, Japan). Additionally, the compressive strength of resole and resole/cellulose composites was tested using the Compressive Strength Testing Machine (Harrish and Terriesh, India). Compressive strength was calculated using equation (1) [18]:

$$Compressive\ strength = \frac{Breaking\ Load\ (N)}{Cross\text{-}sectional\ area\ (cm^2)} \quad \ldots\ldots\ldots\ldots\ldots (1)$$

For this study, cubic-shaped composites, and pure resole resin were subjected to compressive strength testing at room temperature, using specimens with approximate dimensions of 2 cm.

Results and Discussion

XRD Analysis of Synthesized Cellulose Powder and Resole/Cellulose Composites

The phase composition and structure of the cellulose powder were characterized by X-ray diffraction (XRD). XRD provides information about the crystal thickness and the crystallinity index of the cellulose. **Fig. 1** shows the XRD patterns of synthesized cellulose, resole resin, and composites within a 2θ range from 20-80 degrees. The main Miller indices (hkl) for nanometer-sized cellulose, (200) and (004),

correspond to Bragg's peaks at 22.9° and 34.6°, respectively. The XRD pattern displayed a strong peak at (200), while the diffraction peak at (004) was very weak. The presence of these peaks in the spectra indicates the crystalline nature of the synthesized cellulose. The observed peaks at 22.9° and 34.6° for cellulose are consistent with the cellulose I crystalline structure reported by Xie et al. [10].

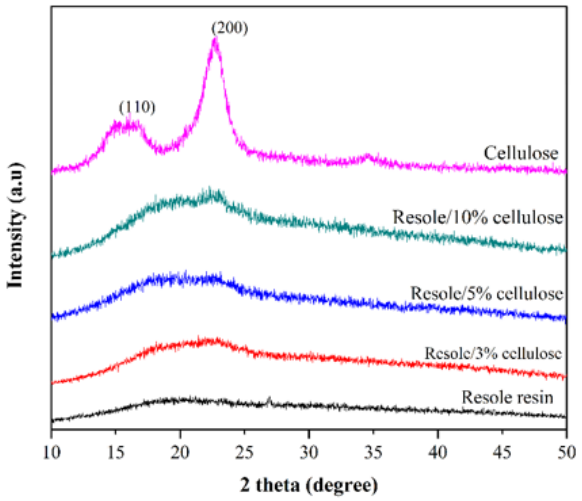

Figure 1: *XRD pattern of synthesized cellulose fiber, resole resin, resole/cellulose composites*

The (200) peak from the XRD pattern was used to calculate the cellulose nano-size using the Debye-Scherrer equation. The crystallite size of cellulose powder obtained from *Sabai* grass was 3.84 nm. The crystallinity index (CI) was calculated using the following equation:

Crystallinity Index (CI) = $(I_{max}- I_{min})/I_{max}$

The synthesized cellulose from *Sabai* grass exhibited a crystalline structure. Thus, the crystallinity index of the cellulose synthesized was found to be 0.766, higher than the CI of microwave-liquefied bamboo (70.6%) [10]. In **Fig. 1**, the XRD patterns of the resole resin and its composites did not show significant peak intensities, indicating that the resole resin and composites were amorphous. The amount of cellulose fiber in the resin was not significant enough to be detected by XRD. However, in the case of 10% cellulose fiber in resole resin, there was a noticeable change compared to pure resole resin, resembling the nature of cellulose fiber. This indicated that the amount of cellulose could be traced by XRD. Thus, the resole resin and its composites were amorphous, and the low amount of cellulose fiber did not contribute significantly to the XRD patterns.

FTIR Analysis of *Sabai* grass, Cellulose Fiber, and their composites

The FTIR spectra of untreated *Sabai* grass and synthesized cellulose are shown in **Fig. 2**. The FTIR spectra of untreated and treated *Sabai* grass fibers, showing distinct differences, and highlighting the peaks at different wavenumbers. Many bands in the spectra (3321, 2896, 1735, 1628, 1506, 1456, 1329, 1166, 1026, and 904 cm^{-1}) match those in the reference spectra for untreated and treated cellulose fibers and are in close agreement with the same references [8-11].

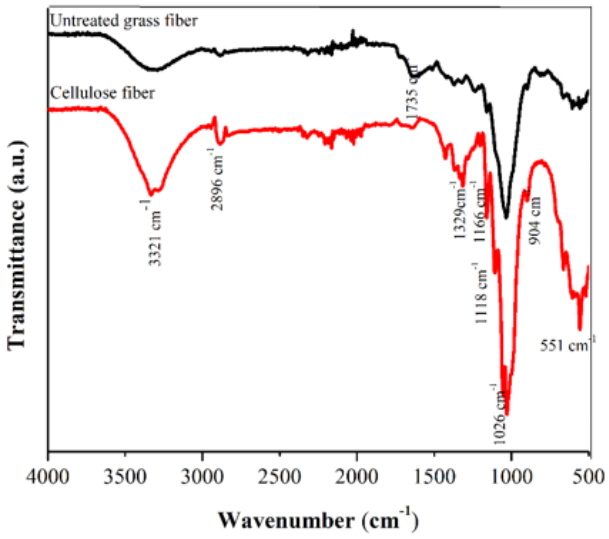

Figure 2: *FTIR spectra of untreated Sabai grass fiber and chemical-treated cellulose fiber*

Table 1 lists the wavenumbers and their corresponding functional groups.The spectral band at 3321 cm^{-1} is characteristic of O-H stretching intramolecular hydrogen bonds. The intensity of the O-H band in chemically treated

cellulose is stronger compared to untreated *Sabai* grass fiber. The band at 2896 cm^{-1} corresponds to C-H stretching. The peak at 1735 cm^{-1}, present in untreated *Sabai* grass fiber but absent in treated cellulose, indicates acetyl and uronic ester groups or ester linkages of ferulic and p-coumaric acid in hemicelluloses, confirming their removal during chemical treatment. Thus, the removal of the peak at 1735 cm^{-1} confirms the elimination of hemicellulose in treated cellulose fiber. The absorption bands at 1628 cm^{-1} and 1506 cm^{-1}, attributed to H-OH stretching vibrations of absorbed water in carbohydrates and aromatic skeletal ring vibrations, are absent in cellulose fiber, confirming the removal of absorbed water and lignin. The bands at 1456 cm^{-1} and 1329-1312 cm^{-1} are due to C-H deformation combined with aromatic ring vibration, C-H stretching, and CH_2 bending, respectively, and show increased intensity in cellulose fiber. The bands at 1166 cm^{-1} and 1118 cm^{-1} are due to C-O-C stretching attributed to β-(1→4) glycosidic linkage and C-OH skeletal vibration, which are more distinct in the spectra of cellulose fiber.

An increase in intensity at 1026 cm^{-1} confirms higher cellulose content. Sharp bands at 904 cm^{-1} and 669 cm^{-1} represent glycosidic C1-H deformation with ring vibration and OH bending, characteristic of β-glycosidic linkages between glucose units in cellulose and O-H out-of-phase bending, respectively. This result indicates the removal of lignin and hemicelluloses through bleaching and alkali treatments without disturbing the cellulose structure in *Sabai* grass fiber [8-11].

The FTIR spectra of pure resole and the resole resin/cellulose composite are shown in **Fig. 3**. Both spectra exhibit similar features with varying intensities. The absorbance band at 3354 cm^{-1} corresponds to O-H stretching. The peak at 1611 cm^{-1} indicates C=C aromatic ring vibrations, which are more pronounced in the pure resin. The spectral band at 1459 cm^{-1} is attributed to the C=C benzene ring, influenced by the $–CH_2–$ methylene bridge.

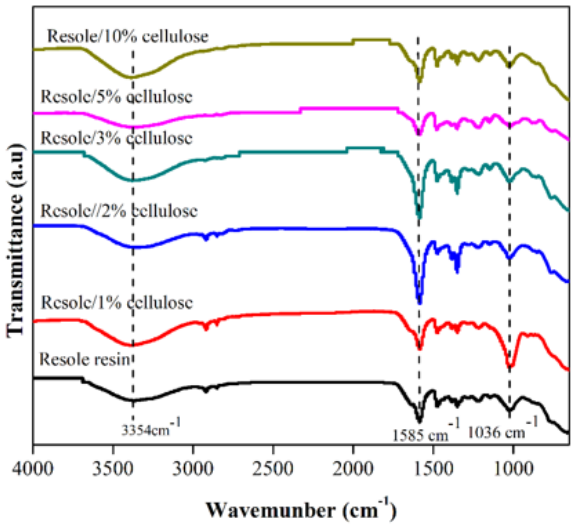

***Figure 3**: FTIR spectra of pure resole resin and resole/cellulose composite*

Table 1: Wavenumber with its corresponding functional group [8, 10, 11]

Wavenumber (cm^{-1})	Functional group
3321	O-H stretching intra-molecular H-bonds
2896	C-H stretching
1735	Acetyl or uronic ester groups or ester linkage of the carboxylic group of ferulic and p-coumaric acid of hemicelluloses
1628	H-OH stretching vibration of absorbed water in carbohydrate
1506	Aromatic skeletal vibration
1456	C-H deformation combined with aromatic ring vibration
1329	C-H stretching and CH_2 bending
1166	C-O-C stretching attributed to β-(1→4) glycosidic linkage

Additional peaks at 1341 cm^{-1}, 1222 cm^{-1}, and 1036 cm^{-1} correspond to OH in-plane vibrations,

asymmetric stretch of phenolic C-C-OH, and single-bond C-O stretching vibrations of the CH_2OH group, respectively. These spectral features are characteristic of phenolic dominant compounds [12]. The absence of new bonds in the composite material confirms that no chemical bonding occurs between the resole resin and cellulose. Instead, cellulose is likely dispersed within the resole resin matrix through physical means which indicates physical dispersion of cellulose within the resin

Mechanical Strength of Resole Resin/ Cellulose Composites

Compressive strength is a mechanical test commonly used to assess a material's ability to withstand loads that tend to reduce its size. This property is typically measured by plotting the applied force against the resulting deformation in a testing machine.

Table 2: The compressive strength of resole/cellulose composites

S.N.	Cellulose (wt.-%)	Breaking load (N)	Surface area A (cm^2)	Compressive strength (MPa)
1	0	592	3.723	15.593
2	1	758.5	4.391	16.942
3	2	962	4.000	23.585
4	3	1073	4.165	25.265
5	5	906.5	5.135	17.310
6	10	592	5.270	11.057

Table 2 presents various parameters of compressive strength for different compositions of resole/cellulose composite. The breaking load, surface area, and compressive strength are organized neatly in the table, corresponding to the wt.-% of cellulose content in the resole resin. The breaking load data for samples - pure resin, 1 wt.-%, 2 wt.-%, 3 wt.-%, 5 wt.-%, and 10 wt.-% resole/cellulose composites - are 592, 758.5, 962, 1073, 906.5, and 592 N, respectively. Similarly, the compressive strength values for each sample are 15.59, 16.94, 23.58, 25.26, 17.31, and 11.05 MPa, respectively. The data illustrates that higher breaking loads correspond to higher compressive strengths. The relationship between compressive strength and cellulose content (Wt.-%) in the composite is depicted in **Fig. 4**.

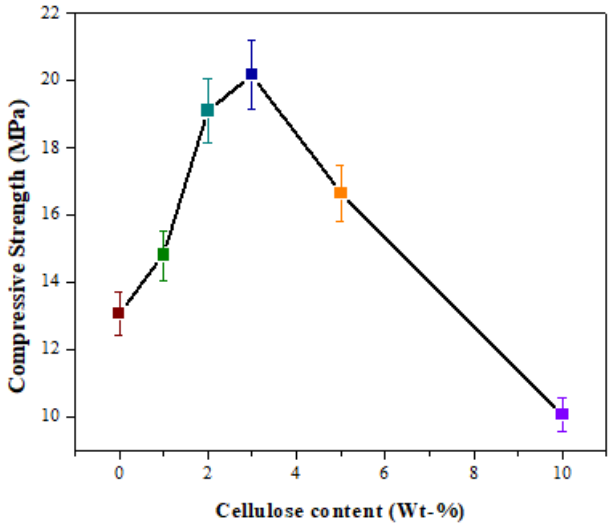

Figure 4: *A plot of compressive strength against cellulose content of resole/cellulose composites*

Fig. 4 shows the compressive strength of different composites when filler materials are incorporated into resole resin. An increase in the mechanical properties of the composites was anticipated [13]. The plots in Figure 4 illustrate that the compressive strength increases with the percentage of cellulose by weight, up to 3 wt.-%. However, the compressive strength decreases when 5 wt.-% and 10 wt.-% cellulose by weight are incorporated. The increase in mechanical strength of the resole/cellulose composite up to 3 wt.-% cellulose fiber loading is due to the homogeneous dispersion of cellulose in the polymer matrix. In contrast, the decrease in mechanical strength for the 5 wt.-% and 10 wt.-% resole/cellulose composites is attributed to the clumping of the loading material. This clumping results from the strong affinity of hydrogen bonds, leading to increased crudity and decreased mechanical strength [4]. The compressive strength of epoxy/ZrO_2 composite [19], cement/silica nanocomposite

[20], and urea-formaldehyde/MgO composites [21] have been investigated in different wt.-% ratio also indicated that the strength depends on the nature of the matrix and filler of their composites. Therefore, the compressive strength of resole/cellulose nanocomposites with 1 wt.-%, 2 wt.-%, and 3 wt.-% cellulose is higher than that of other composites. The decline in strength at 5 wt.-% and 10 wt.-% cellulose is likely due to agglomeration, as indicated by the increased viscosity and poor dispersion.

SEM Analysis of Cellulose Fiber, Resole Resin, and its Composites

SEM was used to analyze the morphological structure of cellulose fiber and resole/cellulose fiber composites, comparing them to raw *Sabai* grass and pure resole resin, respectively in **Fig. 5. Fig. 5(a)** shows the SEM image of raw Sabai grass, revealing a very rough surface with numerous adhered substances. **Fig. 5 (b)** depicts the SEM image of extracted cellulose fiber from Sabai grass, where a reduction in fiber diameter to around 50 µm is observed. The smooth surface of the cellulose fiber confirms the removal of lignin, hemicellulose, ashes, and other impurities through chemical treatments like bleaching and alkaline treatment. **Fig. 5 (c)** displays the SEM image of pure phenol-formaldehyde resin, which exhibits a compact structure with glass-like fracture patterns. **Fig. 5 (d)** presents the SEM image of the resole/cellulose fiber composite, showing surface modifications due to the addition of cellulose fiber. The increased mechanical strength of the composites can be attributed to the interfacial attraction between the cellulose fiber and the phenolic resin. The interfacial bonding between the cellulose fiber and the resole resin restricts the movement of resin segments, resulting in reduced deformations [18]. The smooth surface of cellulose fibers and the modified surface morphology of the composites confirm the successful incorporation of cellulose into the resin.

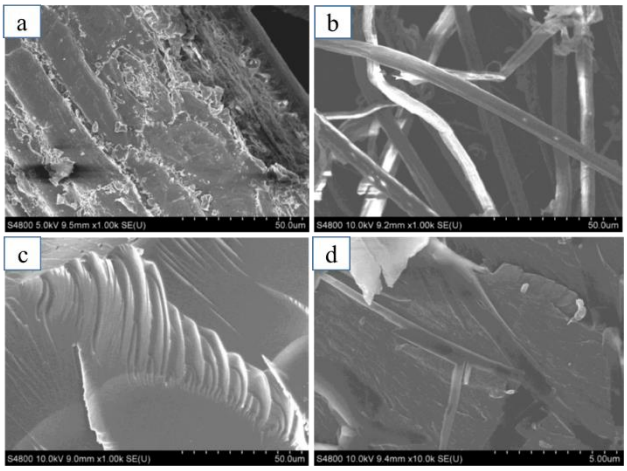

Figure 5: *SEM images of a) raw Sabai grass b) cellulose fiber c) pure resole resin d) resole/1wt.-% cellulose fiber composite*

Conclusions

In this study, cellulose fiber was isolated from Sabai grass using mechanical and chemical treatments. The prepared cellulose fiber was characterized using X-ray diffraction (XRD), scanning electron microscopy (SEM), and Fourier-transform infrared spectroscopy (FTIR). The synthesized cellulose fiber was then mixed with resole resin at varying wt.-% of cellulose. The resulting resole/cellulose composites were evaluated using compressive strength tests (CST).The XRD spectra revealed that the isolated cellulose fibers have a nanometer-range diameter and crystalline structure, with a crystallite size of 3.8 nm and a crystallinity index of 0.766. FTIR analysis showed the removal of lignin and hemicellulose from the cellulose fiber compared to untreated *Sabai* grass fiber. The FTIR spectra of pure resole and resole/cellulose composite were similar, indicating that cellulose and resole do not form chemical bonds and that cellulose is physically dispersed within the resole matrix.Compressive strength testing revealed that the compressive

strength of the resole/cellulose resin composite increased with up to 3 wt.-% cellulose fiber loading. This improvement is attributed to the interfacial bonding between the cellulose and the polymer matrix. However, the compressive strength decreased at 10 wt.-% cellulose loading due to agglomeration and poor chemical bonding between the organic filler (cellulose) and the resole resin.

Future work could explore optimizing cellulose fiber dispersion methods and investigating the use of coupling agents to improve the interfacial bonding between cellulose and resole resin. Additionally, the potential applications of these composites in various industries warrant further investigation.

Acknowledgements

The authors would like to acknowledge Dr. Lok Kumar Shrestha, Research Center for Materials Nanoarchitectonics (MANA), National Institute for Materials Science (NIMS), Japan for the support of characterization of XRD and SEM analyses. We thank the Centre for Material Testing Laboratory, Pulchowk Campus, Lalitpur for a compressive strength test.

Author(s) Contribution Statement

A. Puri: Investigation, Data curation, Formal analysis, Writing-original draft preparation, and Software, **R. Pandit:** Conceptualization, Methodology, Software, Validation, Formal analysis, Writing-original draft preparation, Supervision and **R. Adhikari:** Writing-review and editing.

Conflict of Interest

The authors do not have any conflict of interest pertinent to this work.

Data Availability Statement

The data that support the findings of this study can be made available from the corresponding author, upon reasonable request.

References

1. A. C. O'Sullivan, Cellulose: The structure slowly unravels. *Cellulose* 1997, 4, 173-207. (DOI. /10.1023/A:1018431705579)

2. A. Khandual, S. Sahu, Sabai Grass: Possibility of Becoming a Potential Textile. In: Muthu, S., Gardetti, M. (eds) Sustainable Fibres for Fashion Industry. *Environmental Footprints and Eco-design of Products and Processes. Springer,* Singapore. 2016, 45-61. (DOI. /10.1007/978-981-10-0566-4_4)

3. D. Aydemir, Morphological and thermal properties of cellulose nanofi brils reinforced epoxy nanocomposites, *Drvna Industrija* 2015, 66 (1), 35-40. (DOI: /10.5552/drind.2015.1403)

4. S.C. Bajia, P. Swarnkar, S. Kumar and B. Bajia, Microwave assisted synthesis of phenol-formaldehyde resin, *E-Journal of Chemistry* 2007, 4, 457-460. (DOI: /10.1155/ 2007/504343)

5. A. Dorieh, N. Ayrilmis, M. F. Pour, S. G. Movahed, M. V. Kiamahalleh, M. H. Shahavi, H. Hatefnia, M. Mehdinia, Phenol formaldehyde resin modified by cellulose and lignin nanomaterials: review and recent progress, *International Journal of Biological Macromolecule*, 2022. 222, B, 1, 1888-1907. (DOI: /10.1016/j.ijbiomac.2022.09.279)

6. J. George and S.N. Sabapathi, Cellulose Nanocrystals: Synthesis, Functional properties and applications, *Nanotechnology, Science and Applications,* 2015, 8, 45–54. (DOI: /10.2147/NSA.S64386)

7. S. Kalia, A. Dufresne, B. M. Cherian, B. S. Kaith, Luc Av´erous, J. Njuguna, and E. Nassiopoulos, Cellulose-based bio- and nanocomposites: a review *International Journal of Polymer Science,* 2011, 837875, 35 pages. (DOI: /10.1155/2011/837875)

8. S. Panthapulakkal, & M. Sain, Preparation and characterization of cellulose nanofibril films from wood fibre and their thermoplastic polycarbonate composites, *International Journal of Polymer Science,* 2012, 1-6. (DOI: /10.1155/2012/381342)

9. F. K. Liew, S. Hamdan, Md. R. Rahman, M. Rusop, Thermomechanical properties of jute/bamboo

cellulose composite and its hybrid composites: the effects of treatment and fiber loading, Advances *in Materials Science and Engineering,* 2017, 1-10. (DOI: /10.1155/2017/8630749)

10. J. Xie, C.Y. Hse, C. F. De Hoop, T. Hu, J. Qi. and T. F. Shupe, Isolation and characterization of cellulose nanofibers from bamboo using microwave liquefaction combined with chemical treatment and ultrasonication, *Carbohydrate Polymers,* 2016, 151, 725–734. (DOI: /10.1016/j.carbpol.2016.06.011)

11. J. Tang, K. Chen, J. Xu, J. Li and C. Zhao, Effects of dilute acid hydrolysis on composition and structure of cellulose in *Eulaliopsis binate*, *Bioresources* 2011, 6(2), (DOI: 1069-1078. BioRes_06_2_1069)

12. A. Thakur, R. Purohit, R. Rana, D. Bandhu, Characterization and evaluation of mechanical behavior of epoxy-cnt-bamboo matrix hybrid composites, *Materials Today Proceeding,* 2018, 5, 3971–3980. (DOI: /10.1016/j.matpr.2017.11.655)

13. W. Liu, A. K. Mohanty, L. T. Drzal, P. Askel, M. Misra, Effects of alkali treatment on the structure, morphology, and thermal properties of native grass fibers as reinforcements for polymer matrix composites, *Journal of Materials Science,* 2004, 39, 1051 – 1054.

14. W. Z. W. Zahari, R. N. R. L. Badri, H. Ardyananta, D. Kurniawan, F. M. Nor, Mechanical properties and water absorption behavior of polypropylene / ijuk fiber composite by using silane treatment, *Procedia Manufacturing,* 2015, 2, 573 – 578. (DOI: /10.1016/j.promfg.2015.07.099)

15. C.A.S. Hill, H.P.S. Abdul Khalil, M. D. Hale, A study of the potential of acetylation to improve the properties of plant fibres, *Industrial Crops and Products,* 1998, 8, 53–63. DOI: /10.1016/S0926-6690(97)10012-7

16. M. C. Matias, M. U. De La Orden, C. G. Sanchez, J. M. Urreaga, Comparative spectroscopic study of the modification of cellulosic materials with different coupling agents, *Journal of Applied Polymer Science*, 2000, 75, 256–266. DOI: /10.1002/(SICI)1097-4628(20000110)75:2%3C256::AID-APP8%3E3.0.CO;2-Z

17. T.G.Y. Gowda, M.R. Sanjay, K. Subrahmanya Bhat, P. Madhu, P. Senthamaraikannan and B. Yogesha. Polymer matrix-natural fiber composites: an overview, *Cogent Engineering* 2018, *5,* 1-13. (DOI: /10.1080/23311916.2018.1446667)

18. C. Wei, H. Liu, A. Qin, W. Wang, Mechanical properties of phenol/formaldehyde resin composites reinforced by cellulose microcrystal with different aspect ratio extracted from sisal fiber. *Polymer Advanced Technology* 2016. (DOI: /10.1002/pat.3831)

19. M. Bishwokarma, A. Bhujel, M. Baskota, and R. Pandit, Green Synthesis of zirconia (zro2) nanoparticles using curcuma longa extract and investigation of compressive strength of epoxy resin (ep)/zro_2 nanocomposites, *Journal of Nepal Chemical Society*, 2021, 42, (1), 45–50. (DOI: /10.3126/jncs.v42i1.35328).

20. S. Basnet, S. Shah, R. Joshi, and R. Pandit, Investigation of compressive strength of cement / silica nanocomposite using synthesized silica nanoparticles from sugarcane bagasse ash, *International Journal of Nanoscience and Nanotechnology*, 2022, 18, (2), 93–98.

21. S.K.C., N. Rai, S. Shah, R. Joshi, N. Raut, S. Shrestha Pradhanang, R. Pandit, influence of magnesium oxide nanoparticles on the compressive strength of urea formaldehyde resin, *Journal of Nepal Chemical Society,* 2022, 43, (1), 95-101. (DOI: /10.3126/jncs.v43i1.46959)